A New Decentralized Control Scheme for Improving Frequency Stability in Islanded Micro-grids

Morteza Afrasiabi [1,*] and Esmaeel Rokrok [1]

[1] *Department of Electrical Engineering, Lorestan University, Khoramabad, Iran*
**Corresponding author: afrasyabi.mo@fe.lu.ac.ir*

Manuscript received 9 April, 2018; Revised 01 February, 2019; accepted 13 February, 2019. Paper no. JEMT-1804-1078.

Usually micro grids (MGs) are portion of low voltage distribution feeder including two type sources: slow response for frequency control such as micro turbine (MT), diesel generator, fuel cell (FC) and fast dynamic response source such as battery storage systems (BSSs) that can play an important role in restoring balance between supply and demand. In this paper, a new decentralized method for enhancement power sharing between distributed generation resources (DGs) is presented for transient stats in the islanded MGs. This method by changing the conventional droop characteristic of DGs in load variation times improves the MG stability with no communication link. The overload (OL) ability of the BS is employed for fast handling of the frequency control at transient times of loads variation. To achieve this purpose, by considering the batteries OL characteristic and slow dynamic of some sources, a new power control scheme is developed for improving power sharing. Using the introduced mechanism, load variations in the MG is automatically detected and the proposed controller acts during transient times until the output power of the prime movers in the slow DGs reaches to the final value. Based on this scheme, the MG ability can be increased to deal with all types of load-changing scenarios. In order to evaluate the proposed pattern, a sample MG has been simulated under the Matlab Simulink environment. The simulation results are well illustrated the improvement of the power sharing and frequency stability in the MG.

Keywords: *Distributed generation, Power sharing, Droop control, Battery storage.*

http://dx.doi.org/10.22109/jemt.2019.126624.1078

Nomenclature

MTDC	Multitier decentralized control
LLC	Local load controller
DTSMC	Distributed terminal sliding mode controller
DES	Distributed energy source
SoC	State of Charge
DSSC	Distributed storage secondary controller
DSs	Distributed storages
IBDG	Inverter based DG
SG	Synchronous generator
VSCs	Voltage source converters
ESS	Energy storage system
LPF	Low-pass second-order filter
MGs	Micro grids
MT	Micro turbine
FC	Fuel cell
BSS	Battery storage system
DG	Distributed generation
OL	Overload

1. Introduction

The growing use of distributed generation resources has been put the new future forward the electrical distribution systems. The profitability of utilizing renewable energy resources such as wind and solar, or predictable resources such as fuel cells and micro turbine, causing attention to problems of energy production to be inevitable in these systems [1-3]. Creating active distribution networks along with decentralized production is another consequence of new structure in the electrical networks. The concept of the MG is also shaped in this new scheme which represents a set of distributed resources and electrical loads with ability to operate islanded from the main grid [4].

The MGs can be connected to the main grid depending on their design and contribute to the improvement of power quality or energy sales within the electricity market framework [5,6]. On the islanded MGs, existing resources in the network are responsible for providing energy. In this case, the performance of the DGs should be controlled in such a way that the required power by loads be properly shared between the existing resources. So that the power sharing should be done according to the capacity of resources appropriately and the stability of the MG must also be maintained [7].

Droop control is the conventional method for suitable power sharing among production units in the electrical networks. This method like to the communication lines, receives information about the frequency and voltage of the MG without the use of physical communication platforms and divides the existing loads appropriately between the resources. The task of the droop controller is the same as governor and actuator in the synchronous generators. In this controller, using the characteristic of the droop, the reference voltage and frequency are determined for DGs [8,9].

Because in the islanded state, the producing power is limited to DGs, these resources should have high flexibility in responding to the load variations. Otherwise, the stability of the MG in the islanded mode due to the lack of an infinite source will be very fragile. Most DGs technologies have a converter for connecting to the electrical distribution systems [10]. In the case that inverter-based distributed generations provide fast-turning power control to the MG, shortage of sufficient capacity for providing instantaneous power at the time of load variations is a serious challenge [11,12].

Some of DGs prime movers due to the dynamic interaction in their mechanism, have a relative slow response in the power generation. When the MG loads are increased, the output power of inverters is increased rapidly; however, primary sources such as MT or FC are limited by insufficient dynamic performance for load tracking [13]. It causes the DC voltage of DG inverters to decrease, which could affect the appropriate performance of DGs and consequently the MG stability collapses. In order to increase stability margin in islanded MGs which are controlled using droop control method, many studies have been done recently. For example, in order to maintain system stability, supply the network demands, and regulate parameters such as frequency, a MTDC scheme that includes three control subsections, is proposed in [14]. To enhance the MG stability, this work suggests LLCs for the network loads and the dump-loads. Each load is equipped with an LLC and a relay to shed or return to the network, which will increase the cost of this method. In this regard, in order to integrate a direct current vector control mechanism with the droop control method to maintain MG voltage and frequency stability in islanded operation conditions a method is suggested in [15]. Compared to the previous methods, the proposed method improves MG stability, reliability, and power quality. This method is applicable for MGs with central control unit and communication links.

In [16], the secondary control scheme is employed to share the power mismatch, match the SoCs of the DESs, and regulate the frequency and voltage of the MG. The proposed scheme has distributed cooperative architecture, and employs DTSMC for the state regulators, and proportional controller for distributed power-sharing and SoC-matching. Reference [17] investigates the design of robust distributed voltage and frequency control for a self-organized MG. A multi-agent distributed secondary hierarchy is proposed using control Lyapunov function. Power resources are categorized as controllable and uncontrollable DG. Controllable DGs are exchanging information with neighbor DGs through agents at communication layer. The agents communicate to restore the voltage and frequency to their nominal references. In [18], a new DSSC scheme is designed for restoration of the voltage and frequency of a standalone MG, and to provide power-sharing and SoC-balancing, using a distributed cooperative architecture. The cooperative DSs are controllable and exchange the information with neighbor DSs through a communication network. The unknown output power of the uncooperative renewable DG is considered as external disturbance to the DSSC. The proposed schemes in the previous methods organize the controllable DGs, DESs and the uncooperative DGs through the communication link in the MG, which can be a weakness because of the communication connection between the DGs.

In literature review, there is no comprehensive study of MG in presence of important load types and only one kind of load is considered in each article. For this reason, in [19], the MG with droop control is analyzed in presence of different kind of loads. Step change in active demand power, dynamic loads such as induction motors in fault condition, and imbalanced harmonic distorted loads are three types of loads considered in this paper. This research is intended to improve droop-characteristic of DGs according to the different type of loads. Study [20] investigates the transient load-sharing ability of an islanded MG with two IBDGs and a SG during variations in generation and load. Due to slow time constants, SGs in general do not respond as quickly as VSCs, and they can end up supplying only a fraction of the transient load. This can be weakness of the mentioned approach and causes the DG sources with VSCs to exceed their maximum power rating during the transient period. Also, the application of proposed method is only applicable for a particular structure of MG.

Usually, short term energy storage devices such as batteries and super capacitors with fast-response dynamic are used to improve the dynamic of slow resources [21,22]. References [23,24] indicate that a fast-response energy storage module must be included in each DG to provide a constant DC voltage with different primary sources. Installation of ESS in each DG is very costly. Hence, some papers focus on installing one ESS for the whole MG. References [25] and [26] study the MG with hybrid distributed generation resources and a central ESS. Although in all of these methods the utilization of the batteries overload capability has been ignored. In another case, slow-dynamic DGs use hybrid along with faster resources such as wind and solar, that the uncertainty in wind speed and solar radiation reduces the reliability of such systems [27,28].

In this paper, a new scheme is proposed to improve the power sharing in the islanded MGs. In this pattern, a new cooperative control strategy is proposed for a MG with fast response DGs and slow DGs. The proposed method does not require to communication link and guarantees the stability of the MG by using the overload feature of the BSs in the MG. the output power of slow-dynamic resources during the initial moment of load change, compensates with the using of batteries overload characteristic and the balance of production and consumption is well established. To achieve this goal, a new adaptive droop characteristic method is employed for active power sharing between MG resources. The proposed method increases the power system stability and security, which helps the integration of distributed renewable energies. The rest of the paper is organized as follows. In second part of the paper, conventional droop control is described. The proposed droop characteristic is explained in section 3 and section 4 shows the analysis of the system dynamic. A sample MG is simulated in section 5 and conclusions are given in section 6.

2. Conventional droop control

When the MG connects to the main grid, the frequency and voltage of MG are adjusted by the main grid. Although in the disconnected mode, its voltage and frequency may vary quickly because of the low inertia and small-time constants of DGs. For appropriate operation of islanded MG, developing proper control scheme is very important in order to keep its voltage and frequency. If several DGs participate in the voltage and frequency tuning, voltage-droop and frequency-droop control strategies can be used to divide power between DGs. Active power-sharing between DGs using droop strategy is calculated based on their droop equation as follows:

$$m_1.P_1 = m_2.P_2 = \cdots = m_n.P_n \quad \textbf{(1)}$$

Where P_n and m_n are active power and droop coefficient of the nth DG, respectively. The droop coefficient of each resource is determined based on its optimum production capacity at the nominal frequency.

Based on droop characteristic presented in Eq. (1) after that altering, the droop controllers change the frequency of all DGs in the islanded mode and after a few seconds, the output powers of DGs are shared based on the droop gains. Considering that some resources, such as FC and MT, have a slow response in power generation, during this time, output power of these sources varies slowly based on its dynamic performance. If MG does not have a short-term energy storage system such as BS, therefore frequency stability of the MG is threatened in the presence of these slow resources. To solve this problem, the proposed droop characteristic is presented in this article, which is described in the third section.

3. The proposed method for power sharing

In this paper, the power sharing strategy enhances with a new cooperative control method in a MG with two types of recourses: slow dynamic resources such as FC and MT and the second category fast resources with BS in their dc links. For this purpose, the BS overload characteristic of fast DGs is considered as the main regulating unit for stable operation of a MG in the islanded mode. In fact, BS due to its very fast dynamic response performs as a spinning reserve for primary frequency control. In the other hand, at the time duration of reaching output power of slow resources from initial operation state to the final operation point, the fast-dynamic resources will be responsible for supply the lack of required energy for electrical loads by using of batteries overload characteristic.

The proposed method is based on the analysis of the behavior of the DGs in confrontation to the load variations. The conventional droop control characteristic is improved basis of this analysis. This method includes two modifications in the present droop technique. The first is related to the droop controller of DGs with BS, and the other is related to the droop controller of slow DGs. These modifications are described in the Fig. 1.

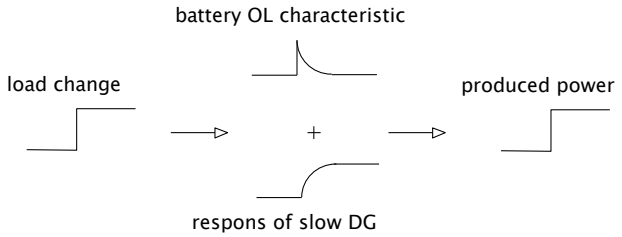

Fig. 1. Concept of proposed control strategy

To test the effectiveness of the proposed approach, a test MG was built based on a system defined by NTUA and used to test proposed control scheme. Complete details of the test system and its power system parameters can be found in [29]. The MG single line diagram was shown in Fig. 2.

The BS, FC and the MT are supposed to be the controllable DG and their inverters are controlled by droop characteristic to feed the load with pre-defined values for voltage and frequency (VSI control) when the main power supply is lost being. All the other inverters operated in PQ control mode to supply a given active and reactive power set-point.

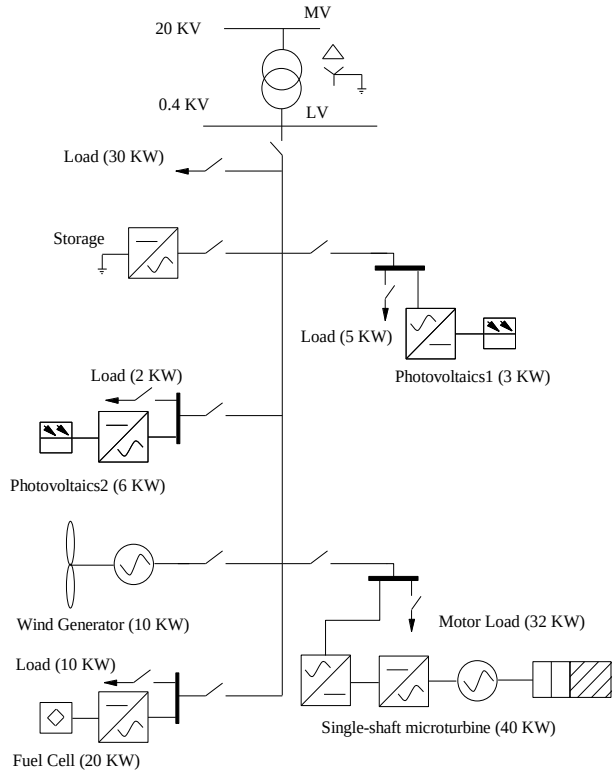

Fig. 2. Single line of MG architecture, comprising DGs and loads.

3.1. Control of the BS

When MG is disconnected from the main grid, the BS output power should be changed quickly while the demand of the MG is varied in order to maintain the network stability. Indeed, the DGs with BS should operate such as slack bus in the general power system. To achieve this goal, the BS system active power droop controller should have a high coefficient gain in steady state. When the load demand is changed, the gain should be reduced quickly and afterwards should be increased gradually to the previous value as illustrated in Fig. 3. High coefficient of the BS active power droop leads the BS system to generate low active power in steady state condition. Subsequently, the low coefficient of active power droop causes the BS to generate or consume approximately all the demand of power variation in dynamic behavior of the MG according to overload characteristic. Usually, due to the existence of fast response resources in the MG, the provision of shortage power in transitional conditions will be assigned to these resources (by change the droop coefficients). Consequently, the active droop gain of BS in the proposed method could be expressed by

$$m_{n,new}(t - t_{alter}) = m_n + (m_{n,new} - m_n)^{-(t-t_{alter})/\tau} \quad \textbf{(2)}$$

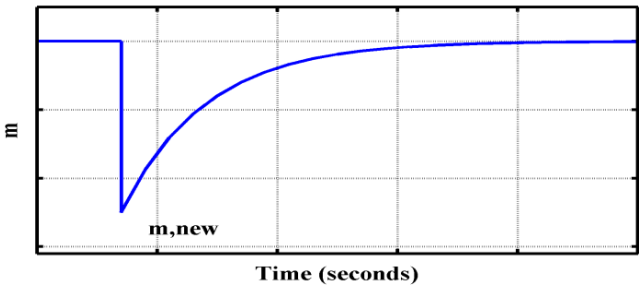

Fig. 3. Frequency droop slope of the BS.

where $m_{n,new}$ and m_n are the new and old droop coefficients; τ is the time constant of the DG system, which shows the speed of changing the droop coefficient from new to old value. The bigger value of τ, leads to the faster change in the droop coefficient and consequently, the lower BS energy supplying. In this equation t_{alter} is the final time that the MG's load is varied and should be identified locally in the BS for decentralized control. When the MG's load is varied, the output powers of all sources are changed followed by this issue. To identify the load changes in the BS locally, the BS output power is compared with its average value in last few moments. If the output power changed abruptly, the instantaneous output power changes relative to its average value and based on this compression, the moment of load change is identified. The average of the power in last few moments $\bar{P}(t)$ is calculated by passing the instantaneous output power P(t) from first order filter with T_d time constant. Afterwards, $\bar{P}(t)$ is calculated from [30]:

$$\bar{P}(t) = \frac{\bar{P}(t-\Delta t).T_d + P(t).\Delta t}{T_d + \Delta t} \quad \textbf{(3)}$$

The last moment that the MG load is varied can be detected based on the above method locally, when (4) is verified:

$$|P(t) - \bar{P}(t)| > \alpha.\min(|P(t)|, |\bar{P}(t)|) \quad \textbf{(4)}$$

In which, ‖ is the absolute value, α is the constant coefficient. Equation (4) uncovers output power changes. This equation computes the difference between the average output power and the instantaneous output power, and compares the result with the minimum of them. If this difference is bigger than a coefficient (α) multiplied by the minimum of instantaneous output power and the average output power, it confirms the instantaneous output power is varied. The α coefficient should be assigned so that all main load changes are identified. The magnitude of α is dependent to T_d and Δt, the larger T_d or the smaller Δt leads to smaller α. To identify this value, the MG should be simulated and the P(t) and $\bar{P}(t)$ should be measured after each critical load change.

3.2. Control of slow DGs

In the slow DGs, output power of the prime mover changes slowly. Therefore, if the output power of the DG inverter changes slowly too, the DC voltage variation of the inverter is reduced which leads to maintain network stability. Therefore, a system should be employed to decelerate the response speed of the inverter. To achieve this purpose, the active power droop coefficient of DGs should be increased when their output active power changes. For this purpose, the DGs droop coefficient is defined as a variable parameter. The proposed structure has been shown in Fig. 4. In order to maintain the frequency stability of the MG, $m_{n,new}$ must be selected so the power assigned to the slow DGs is the same value of its, before of load change. In other words, in the slow sources the output power of the inverter should be changed as the output power of the prime mover to maintain the balance of power both in steady state and in transient state. If the output power of the inverter and prime mover are not equal, in the subsequent DC voltage collapse which results in system instability. Thus, the floating droop coefficient of slow DGs is variable with the time and results in increasing the droop gain in dynamic condition. Determining these values and coefficients after each load change is based on the principles as follows.

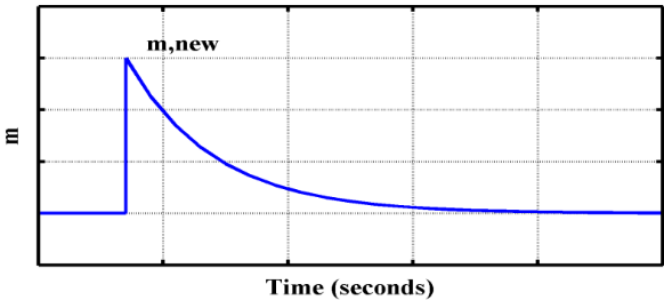

Fig. 4. Frequency droop slope of slow DGs.

3.3. Determining of coefficients

The frequency deflection is created in the MG by the imbalance between load and production. Usually in the conventional power systems, the magnitude of active power variation is proportional to the magnitude of frequency changes [31]. In the synchronous generator machines, the rotor swing equation can be calculated as follows [32,33]:

$$\frac{J_n.d\omega_n}{dt} = P_{Mn} - P_{En} = \Delta P_n \quad \textbf{(5)}$$

Where ω_n is the system frequency, J_n is inertia constant, P_{Mn} is the mechanical prime mover power, P_{En} is the electrical power, and ΔP_n is the unbalance of active power changes. Considering that J_n of synchronous generators can be achieved through data sheet or measurement method, if the $\frac{d\omega_n}{dt}$ after each change is measured, then the ΔP_n of each generator can be calculated, and the sum of ΔP_n can be achieved as follows [34]:

$$\Delta P = \sum_n \Delta P_n \quad \textbf{(6)}$$

For consideration the noise issue in the measurement of df/dt, the average value of the df/dt is used to eliminate the distortion of measured signal. To demonstrate the effectiveness of the proposed method, simulation results are shown in Fig.5 for the mentioned network in the Fig. 2 (when imposing a new load to network). In these figures the averaging time window is considered 100 ms. As can be seen, signal distortion was improved in Fig. 5(c) compared to Fig. 5(b).

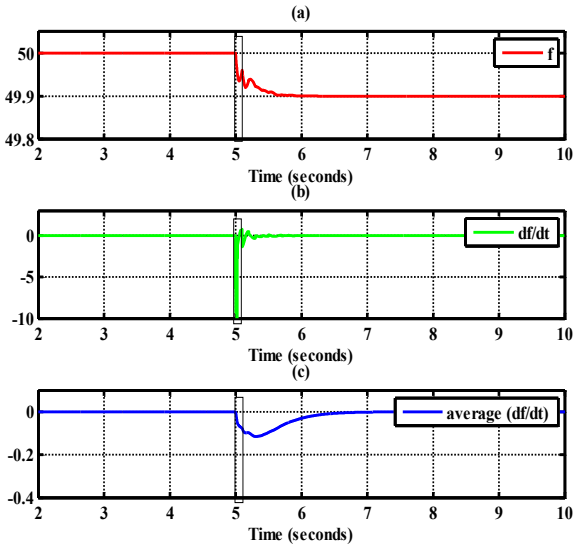

Fig. 5. The measured signals. (a) Frequency. (b) Derivative of the frequency. (c) The average value of df/dt.

Usually in the MGs, it is difficult to identify the equivalent inertia constant J_n of each DG, because of the complex system of different types of DGs. For this reason, it is assumed that all DGs can be considered as a whole source and the MG total equivalent inertia constant can be obtained by simulation method. Afterwards, Eq. (5) can be used to calculate the magnitude of active power change of MG. Considering to the simulation system in the islanded mode, a power unbalance ΔP is added to the MG and the corresponding $\frac{d\omega}{dt}$ and J are identified respectively. Therefor, the MG total equivalent inertia constant J can be obtained as follows:

$$J = \frac{\Delta P}{d\omega/dt} \quad \textbf{(7)}$$

For instance, in micro-grid Fig. 2, after each disturbance, the magnitude of active power deficiency (ΔP) in the MG can be estimated according to (5). This calculated power (ΔP) at the first time should be provided by the battery storage system ($\Delta P_{Bat} = \Delta P$) with changing its droop characteristic as shown in Fig. 6. So, the droop characteristic of the BS changes as follows:

$$m_{Bat,new} = m_{Bat}.\frac{\Delta\omega}{\Delta P} \quad \textbf{(8)}$$

Where, Δω and $m_{Bat,new}$ are the magnitude of frequency change and the new droop coefficient of the BS. Afterwards, the battery power is gradually decreased and the task of supplying power is shared between the controllable resources by changing the droop characteristic as follows (Fig. 6):

$$m_{FC,new} = \frac{\Delta\omega}{\Delta P.\frac{\frac{1}{m_{FC}}}{\sum_i\left(\frac{1}{m_i}\right)}}, \qquad m_{MT,new} = \frac{\Delta\omega}{\Delta P.\ (\frac{1}{m_{MT}})/\sum_i(\frac{1}{m_i})} \quad \textbf{(9)}$$

Where, $m_{FC,new}$, $m_{MT,new}$ and m_i are the new droop coefficients of FC , MT and i-th DG respectively.

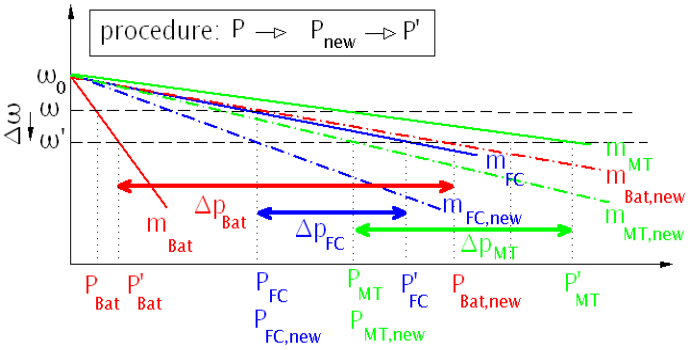

Fig. 6. Droop coefficients change strategy

The maximum allowable droop coefficient of DGs can be achieved according to the allowed domain output power of DGs and frequency change as following equation:

$$0 \le m_i \le \frac{f_{max} - f_{min}}{p_{i,max} - p_{i,min}} \quad \textbf{(10)}$$

Where $p_{i,max}$ and $p_{i,min}$ are the maximum and minimum output active power of the i-th DG, f_{max} and f_{min} are the allowable maximum and minimum value of the frequency. Then, the obtained coefficients should be evaluated by the dynamic stability analysis of the system which is discussed in section 4.

3.4. Battery OL characteristic selection

Use the battery OL feature helps the related DGs to supply the whole demand variations initially in the few initial seconds [35]. Consequently, the BS power rate should be equal to the largest demand changes in the MG. Afterwards, the battery output power reduces gradually, on the other hand the slow DGs increase the rate of their participation in supplying the MG demand slowly. After some seconds, the output of BSs becomes previous operation point, and the demand is shared perfectly between all DGs. It should be noted that at the initial moment of the load change, all of the new demand is almost provided by the ESS (by its very low droop coefficient) and power sharing based on the DGs droop characteristic are used only in the steady-state condition.

In this strategy, overloaded output power of battery should be able to overcome maximum unbalance power which can happen among demand and supply. Maximum unbalance power in the MG can be obtained considering to the average transferred power between the components of MG. The maximum unbalance power can be as shortage or surplus of production. Thus, the required overloaded characteristic of the BS is achieved by the maximum unbalance power in the MG. The proposed algorithm for proper selection of the battery OL characteristic of MG, is shown in Fig. 7 and explained as follows.

1- Considering different scenarios of surplus or shortages power in the MG, such as:

- *Starting the biggest induction motor in the MG.*
- *Disconnect interconnection line while importing/exporting the most power to/from main grid.*
- *Abrupt change in the output power of renewable energy resources such as WT or PV, due to changing in the wind speed and irradiation.*

2- Determine the amount of extra/shortage required energy in the MG to reach a new stable state.

$$W = \int_0^\tau \Delta P.\,dt \quad \textbf{(11)}$$

Where, ΔP and τ are the magnitude of unbalance power and the duration change time, respectively.

3- Calculation the amount of energy changes in the slow resources, according to equation (12).

$$W_{slow\ DG} = \sum_n \int_0^\tau \Delta P_{DG_n}.dt \quad \textbf{(12)}$$

In which, ΔP_{DG_n} is the value of power change in n-th slow resource.

4- Calculate the required power for battery by using of Eq. (11) and Eq. (12).

$$W_{battery} = W - W_{slow\ DG} \quad \textbf{(13)}$$

5- Determine the battery OL feature in charge and discharge mode according to the achieved parameters.

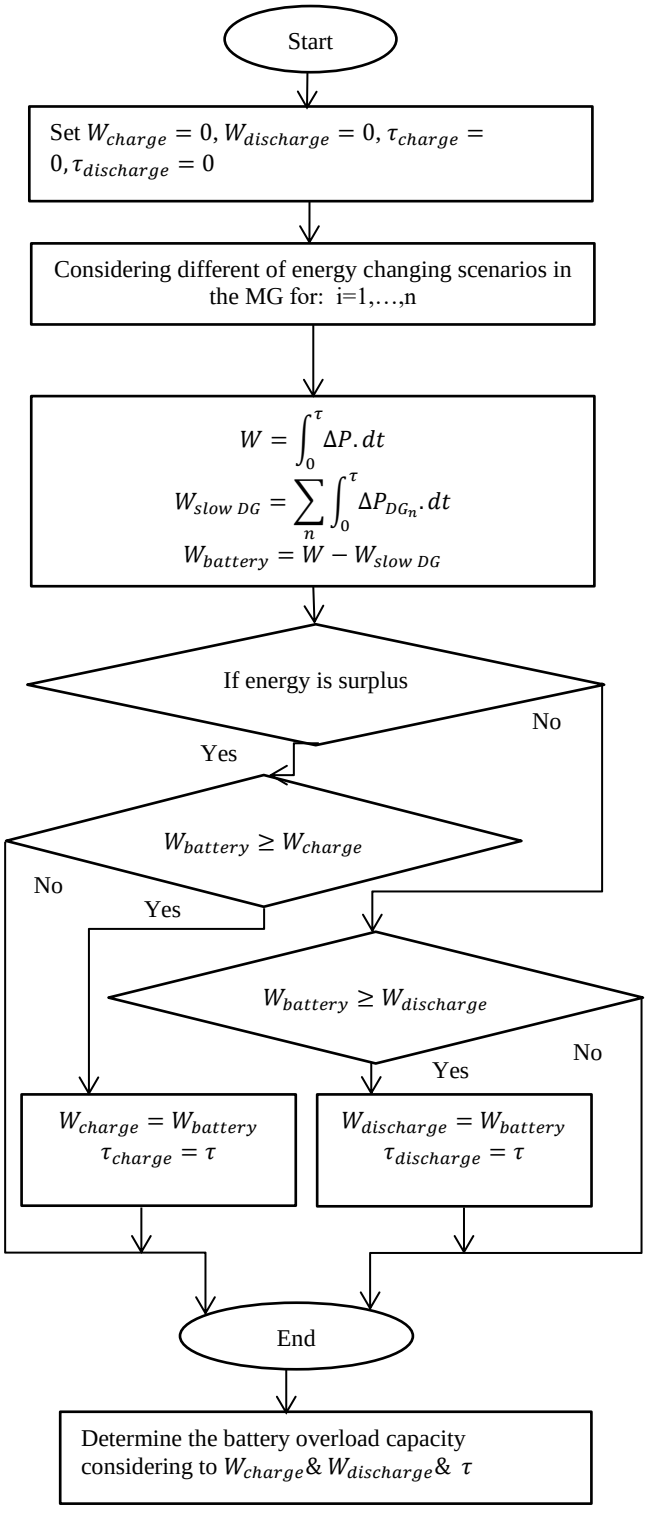

Fig. 7. Appropriate battery overload characteristic selection algorithm

4. System dynamics and control design parameters

In this section, the system-dynamic model and the stability analysis are provided to properly design m coefficients of the PI compensator, corresponding to the active-power injection control loop. When the DGs converter is connected to the grid through the generic impedance, the active and reactive powers injected to the grid can be expressed as follows:

$$P = \frac{EV}{Z} sin\varphi \quad \textbf{(14)}$$

$$Q = \frac{EV}{Z} cos\varphi - \frac{V^2}{Z} \quad \textbf{(15)}$$

Where E is the DG voltage, V is the grid voltage, z is the line impedance and φ is the phase between E and V. A small-signal analysis is provided in order to show the system stability and the transient response. The power-calculation block uses a LPF. Hence, both the power and reactive output power measured from the power-calculation block can be defined as

$$\Delta p_{\text{meas}}(s) = \overbrace{\frac{\omega_0^2}{s^2+2\zeta\omega_0 s+\omega_0^2}}^{LPF}.[(v.sin\varphi.\Delta E(s) + v.E.cos\varphi.\Delta\varphi(s))/z] \quad \textbf{(16)}$$

$$\Delta q_{\text{meas}}(s) = \frac{\omega_0^2}{s^2+2\zeta\omega_0 s+\omega_0^2}.[v.cos\varphi.\Delta E(s) - v.E.sin\varphi.\Delta\varphi(s)/z] \quad \textbf{(17)}$$

where ω_0 is the resonance frequency and ζ the damped coefficient. The lower-case variables with the symbol Δ indicate small-signal values. The variables $\Delta p_{\text{meas}}(s)$ and $\Delta q_{\text{meas}}(s)$ after passing the power controllers be as follows:

$$\Delta\varphi(s) = -\frac{m}{s}.\Delta p_{\text{meas}}(s) \quad \textbf{(18)}$$

$$\Delta E(s) = -n.\Delta q_{\text{meas}}(s) \quad \textbf{(19)}$$

Where, m is the active power droop coefficient and n is the reactive power droop coefficient. A combination of previous relationships

$$\Delta\varphi(s) = -\frac{m}{s}.\frac{\omega_0^2}{s^2+2\zeta\omega_0 s+\omega_0^2}.\left[\frac{v.sin\varphi.\Delta E(s)+v.E.cos\varphi.\Delta\varphi(s)}{z}\right] \quad \textbf{(20)}$$

$$\Delta E(s) = -n.\frac{\omega_0^2}{s^2+2\zeta\omega_0 s+\omega_0^2}.\left[\frac{v.cos\varphi.\Delta E(s)-v.E.sin\varphi.\Delta\varphi(s)}{z}\right] \quad \textbf{(21)}$$

By combining (19) and (20), we can be obtain the following fifth-order characteristic equation:

$$s^5+c_4s^4+c_3s^3+c_2s^2+c_1s+c_0 = 0 \quad \textbf{(22)}$$

Being

$$\begin{aligned} c_4 &= 4\,\omega_0.\zeta.Z \\ c_3 &= V.\,\omega_0{}^2.\cos\varphi.n + 2\omega_0{}^2.(1+2\zeta^2).Z \\ c_2 &= 2V\,.\,\omega_0{}^2.\zeta\,.\cos\varphi.n + \omega_0{}^2.V.E\,.\cos\varphi.m + 4\zeta.\,\omega_0{}^3.Z \\ c_1 &= V\,.\,\omega_0{}^4.\cos\varphi.n + V.\,E.\,\omega_0{}^3.2\zeta\,.\cos\varphi.\,m + \omega_0{}^4.Z \\ c_0 &= V.\,E.\,\omega_0{}^4.\,m.(\cos\varphi + (V/Z).\,n) \end{aligned} \quad \textbf{(23)}$$

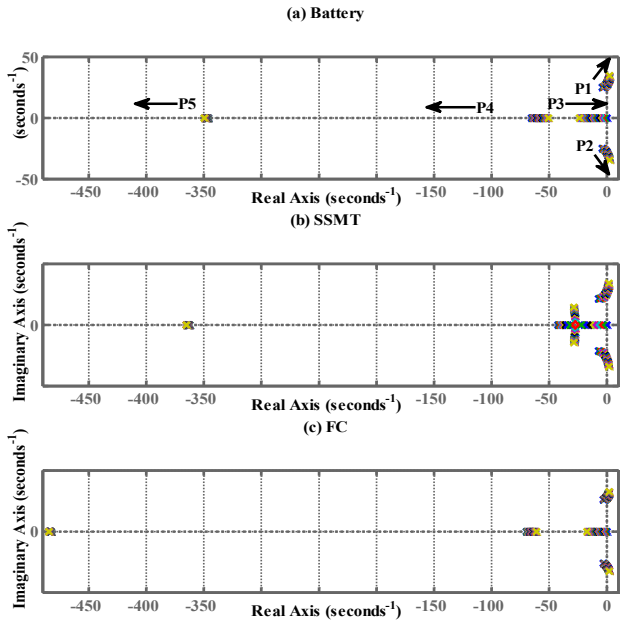

Fig. 8. System root locus for 0.0001 < **m** < 0.01 and n= 0.02. (a) BS. (b) MT. (c) FC.

The system root locus for different droop coefficients is shown in Fig. 8(a), 8(b) and 8(c) for BS, MT and FC. The inverters characteristic equation has five poles of p1 to p5. These figures show the root-locus behavior when m is increased. Note that P3, P4, and P5 are far away from P1 and P2, and P1 and P2 go toward the imaginary axis, becoming a faster oscillatory system. In these figures, when *m* is selected as 0.0095, 0.0061 and 0.0033 in BS, FC and MT, the system has a conjugate pole pair around the imaginary axis, which illustrates a decreased system stability margin and weak damping characteristic. When m is increased to 0.01, the conjugate pole pair is passed from the imaginary axis and the system is unstable in this case for three DGs. Thus, using m it is possible to locate the poles where it is more convenient and we can achieve to the proper value of m in calculation of inverters droop coefficients.

5. Simulation results

The results of two methods are presented in this section. In case 1, in order to evaluate the dynamic behavior of a MG during load Change by proposed scheme, the LV test system presented in Fig. 2 was implemented in a simulation platform under the *Matlab Simulink* environment. In case 2, to evaluate the proposed control system with other strategy, the MG state space equations are modeled in MATLAB. These equations are solved by Newton method for steady state condition. The dynamic response of the MG is obtained by applying trapezoidal rule in these state equations. At the end, two load/generation scenarios using the proposed scheme were tested by two methods, with the corresponding results described next. The related parameters of the simulated system are presented in Table 1 and [29].

Table 1. Parameters of the simulated system.

Symbol	Parameter	Value	Unit
V_{dc}	DC link Voltage of VSC	650	V
L_g, L_f	Filter inductances	0.2,1.8	mH
C_f	Filter capacitor	25	μF
F_s	Switching frequency	10	kHZ
m_{Bat}, m_{FC}, m_{MT}	Active power droop Coefficients	0.009,0.006,0.003	-
n	Reactive power droop Coefficient	0.02	-
$T_d, \Delta t$	Coefficients of time	100,1	mS
α	Coefficient constant	0.3	-
$P_{Bat,max}, P_{FC,max}, P$	Maximum power	33,20,40	kW

5.1. Battery calculation

To achieve a suitable battery capacity by proposed algorithm, it is employed for the study system shown in Fig. 2. Demand, production and shortage or surplus unbalance powers of the MG for the critical cases of uncontrolled changes that are achieved considering to the background of the change power in the MG are shown in Table 2.

Table 2. Critical scenarios of MG power change

Different scenarios	ΔP (KW)	The worst scenarios
Wind Generator power drop	10	
PV power drop	-6	
Motor starting	32	√
Power export to grid	-30	√
Power import from grid	28	

The nominal capacity of the BS is obtained by proposed algorithm for different scenarios, and the worst case is selected as the final power capacity of the BS. The acceptable overload factor, allowed overload duration time and nominal power of the BS are evaluated as 3, 15 sec and 11 kW respectively for this MG. That this shows, three times of battery power (3*11=33 kW) with a length time of 15 seconds in the overload mode covers the worst scenarios of MG power change.

5.2. Evaluate high load scenario

The scenario is characterized by a local load of 78 kW (60% of impedance type and 40% of induction motor type) and a local generation of 48kW (high load scenario). The generation of MT, FC, wind generator, PV1 and PV2 are assumed to be 20, 10, 9, 3 and 6 kW respectively. A fault in the MV side occurred at t=5 sec followed by MG islanding after.

Figures 9 and 10, show the results of MG high load scenario using the proposed pattern. With the new controller immediately after the load variations, the imbalance between production and consumption of power is detected in the first. Then, the task of supplying of identified power is initially assigned to the BS. The power assigned to the FC and MT at the moment of load change are adjusted to the same value as before change. Afterwards, the produced power by the FC and MT gradually increase according to the time constant of their prime mover and consequently the battery power will be reduced. Eventually, the production power of these resources reaches to the final value. In this case, the frequency stability of the MG is maintained, which is the benefits of proposed method.

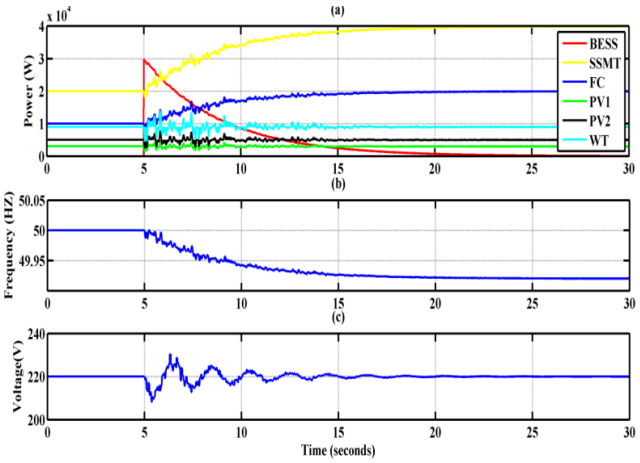

Fig. 9. High load scenario by proposed scheme (simulation). (a) Active output power of the DGs. (b) Frequency of the MG. (c) Voltage of the MG.

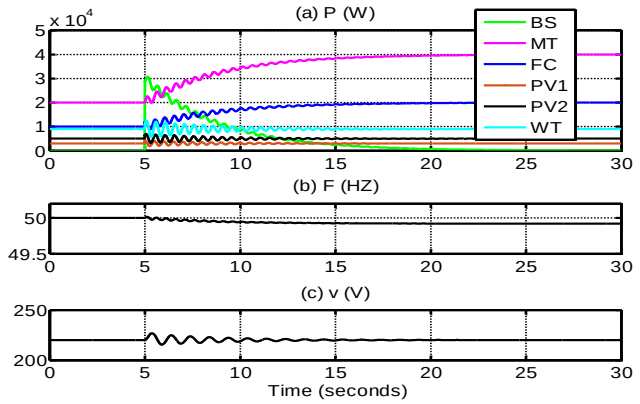

Fig. 10. High load scenario (using the state space equations). (a) Active output power of the DGs. (b) Frequency of the MG. (c) Voltage of the MG.

For the proposed cooperative frequency control method, the reactive power outputs of the DGs can be seen in the Fig. 11. The corresponding reactive power of DGs, can be reached faster to the final value because of the quick action made by the VSCs control system. While, the active power of inverters changes proportional to DGs prime mover speed by the proposed control system.

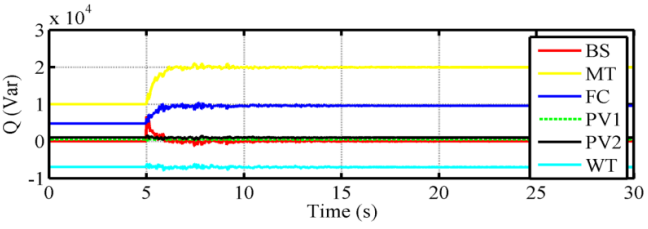

Fig. 11. Reactive output power of the DGs for high load scenario (simulation).

5.3. Evaluate low load scenario

A low load scenario with power being exported to the MV network was also tested. The scenario is characterized by a local load of 48 kW (60% of impedance type and 40% of induction motor type) and a local generation of 78 kW. The generation of MT, FC, wind generator, PV1 and PV2 are assumed to be 40, 20, 11, 3 and 5 kW respectively. Fault conditions are those previously described.

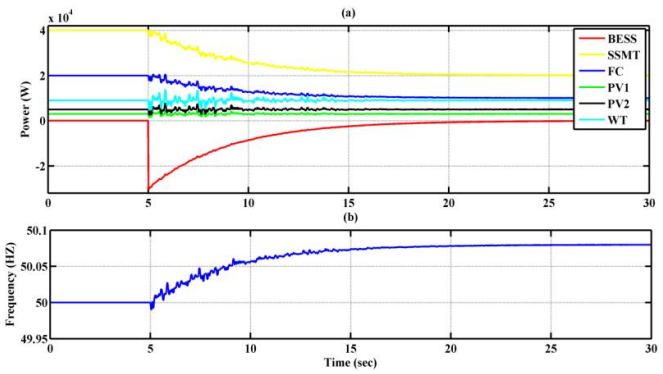

Fig. 12. Low load scenario by proposed scheme (simulation). (a) Active output power of the DGs. (b) Frequency of the MG.

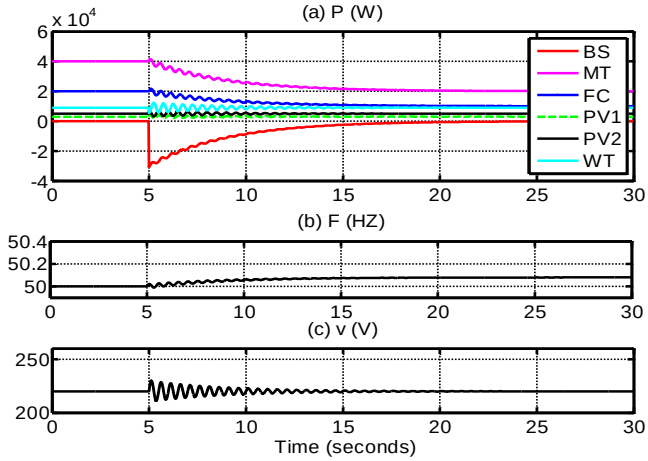

Fig. 13. Low load scenario (using the state space equations). (a) Active output power of the DGs. (b) Frequency of the MG.

In this case, the MG absorbs the power generation surplus after unpredicted system islanding, as can be observed in Figures 12 and 13. In both scenarios (high and low load conditions), a slow frequency restoration process that results from satisfactory of proposed controller can be observed. During this phenomenon, the BS is responsible for a continuous matching between load and generation.

6. Conclusions

Due to the existence of some slow dynamic resources among the DGs of a MG, integration of energy storage elements to supply power during short term disturbances is required to supply transient loads and contribute to MG stability during faults. In this paper a new structure for improving the MG stability by changing the droop characteristic of resources and optimal sizing of a BS for islanded MGs is performed. For this reason, design equations are developed to properly determine the required droop coefficients for resources. Then, was introduced an algorithm which determines the optimal size of overload rates for existing BS. In addition, the design criteria to adequately specify a BS bank meeting the energy requirement is presented and evaluated. The effectiveness of the proposed variable droop method and BS bank design criteria is evaluated through simulations showing good results, allowing the system to ride through short term transient disturbances and load variations.

References

[1] Glinkowski, M., J. Hou, and G. Rackliffe. "Advances in wind energy technologies in the context of smart grid." *Proceedings of the IEEE* 99, no. 6 (2011): 1083-1097.

[2] San M., J. Ignacio, I. Zamora, J. J. S. Martín, V. Aperribay, and P.

Eguia. "Hybrid fuel cells technologies for electrical microgrids." *Electric Power Systems Research* 80, no. 9 (2010): 993-1005.
[3] Srinivas, T., and B. V. Reddy. "Hybrid solar–biomass power plant without energy storage." *Case Studies in Thermal Engineering* 2 (2014): 75-81.
[4] Lasseter, R. H. "Microgrids." In *2002 IEEE Power Engineering Society Winter Meeting. Conference Proceedings (Cat. No. 02CH37309)*, vol. 1, pp. 305-308. IEEE, 2002.
[5] Niu, M., W. Huang, J. Guo, and L. Su. "Research on economic operation of grid-connected microgrid." *Power System Technology* 34, no. 11 (2010): 38-42.
[6] Mizani, S., and A. Yazdani. "Optimal design and operation of a grid-connected microgrid." In *2009 IEEE Electrical Power & Energy Conference (EPEC)*, pp. 1-6. IEEE, 2009.
[7] Katiraei, F., M. R. Iravani, and P. W. Lehn. "Micro-grid autonomous operation during and subsequent to islanding process." *IEEE Transactions on power delivery* 20, no. 1 (2005): 248-257.
[8] Barklund, E., N. Pogaku, M. Prodanovic, C. Hernandez-Aramburo, and T. C. Green. "Energy management in autonomous microgrid using stability-constrained droop control of inverters." *IEEE Transactions on Power Electronics* 23, no. 5 (2008): 2346-2352.
[9] Li, C., E. A. Coelho, M. Savaghebi, J. C. Vasquez, and J. M. Guerrero. "Active power regulation based on droop for AC microgrid." In *2015 IEEE 10th International Symposium on Diagnostics for Electrical Machines, Power Electronics and Drives (SDEMPED)*, pp. 508-512. IEEE, 2015.
[10] Lasseter, R. H. "Microgrids and distributed generation." *Journal of Energy Engineering* 133, no. 3 (2007): 144-149.
[11] Kolluri, R. R., I. Mareels, T. Alpcan, M. Brazil, J. D. Hoog, and D. Thomas. "Power sharing correction in angle droop controlled inverter interfaced microgrids." In *2015 IEEE Power & Energy Society General Meeting*, pp. 1-5. IEEE, 2015.
[12] Majumder, R.. "Some aspects of stability in microgrids." *IEEE Transactions on power systems* 28, no. 3 (2013): 3243-3252.
[13] Saha, A. K., S. Chowdhury, S. P. Chowdhury, and P. A. Crossley. "Modeling and performance analysis of a microturbine as a distributed energy resource." *IEEE Transactions on Energy Conversion* 24, no. 2 (2009): 529-538.
[14] Nourollah, S., A. Pirayesh, and M. Fripp. "Multitier decentralized control scheme using energy storage unit and load management in inverter-based AC microgrids." *Turkish Journal of Electrical Engineering & Computer Sciences* 25, no. 2 (2017): 735-751.
[15] Ramezani, M., and S. Li. "Voltage and frequency control of islanded microgrid based on combined direct current vector control and droop control." In *2016 IEEE Power and Energy Society General Meeting (PESGM)*, pp. 1-5. IEEE, 2016.
[16] Shotorbani, A. M., S. Ghassem-Zadeh, B. Mohammadi-Ivatloo, and S. H. Hosseini. "A distributed secondary scheme with terminal sliding mode controller for energy storages in an islanded microgrid." *International Journal of Electrical Power & Energy Systems* 93 (2017): 352-364.
[17] Shotorbani, A. M., S. Ghassem-Zadeh, B. Mohammadi-Ivatloo, and S. H. Hosseini. "A distributed non-Lipschitz control framework for self-organizing microgrids with uncooperative and renewable generations." *International Journal of Electrical Power & Energy Systems* 90 (2017): 267-279.
[18] Shotorbani, A. M., B. Mohammadi-Ivatloo, L. Wang, S. Ghassem-Zadeh, and S. H. Hosseini. "Distributed secondary control of battery energy storage systems in a stand-alone microgrid." *IET Generation, Transmission & Distribution* 12, no. 17 (2018): 3944-3953.
[19] Khaledian, A., and M. A. Golkar. "Analysis of droop control method in an autonomous microgrid." *Journal of applied research and technology* 15, no. 4 (2017): 371-377.
[20] Klem, A., M. H. Nehrir, and K. Dehghanpour. "Frequency stabilization of an islanded microgrid using droop control and demand response." In *2016 North American Power Symposium (NAPS)*, pp. 1-6. IEEE, 2016.
[21] Mebarki, N., T. Rekioua, Z. Mokrani, D. Rekioua, and S. Bacha. "PEM fuel cell/battery storage system supplying electric vehicle." *International Journal of Hydrogen Energy* 41, no. 45 (2016): 20993-21005.
[22] Belmonte, N., C. Luetto, S. Staulo, P. Rizzi, and M. Baricco. "Case studies of energy storage with fuel cells and batteries for stationary and mobile applications." *Challenges* 8, no. 1 (2017): 9.
[23] Sun, X., Y. Hao, Q. Wu, X. Guo, and B. Wang. "A multifunctional and wireless droop control for distributed energy storage units in islanded AC microgrid applications." *IEEE Transactions on Power Electronics* 32, no. 1 (2017): 736-751.
[24] Li, C., E. Antônio Alves Coelho, T. Dragicevic, J. M. Guerrero, and J. C. Vasquez. "Multiagent-based distributed state of charge balancing control for distributed energy storage units in AC microgrids." *IEEE Transactions on Industry Applications* 53, no. 3 (2017): 2369-2381.
[25] Merabet, A., K. T. Ahmed, H. Ibrahim, R. Beguenane, and A. M. Ghias. "Energy management and control system for laboratory scale microgrid based wind-PV-battery." *IEEE Transactions on Sustainable Energy* 8, no. 1 (2017): 145-154.
[26] Luna, A. C., N. L. Diaz, M. Graells, J. C. Vasquez, and J. M. Guerrero. "Mixed-integer-linear-programming-based energy management system for hybrid PV-wind-battery microgrids: Modeling, design, and experimental verification." *IEEE Transactions on Power Electronics* 32, no. 4 (2017): 2769-2783.
[27] He, M., S. Murugesan, and J. Zhang. "Multiple timescale dispatch and scheduling for stochastic reliability in smart grids with wind generation integration." In *2011 Proceedings IEEE INFOCOM*, pp. 461-465. IEEE, 2011.
[28] Park, J., W. Liang, J. Choi, A. A. El-Keib, M. Shahidehpour, and R. Billinton. "A probabilistic reliability evaluation of a power system including solar/photovoltaic cell generator." In *2009 IEEE Power & Energy Society General Meeting*, pp. 1-6. IEEE, 2009.
[29] S. Papathanassiou. Study-Case LV Network. [Online]. Available: http://microgrids.power.ece.ntua.gr/documents/Study-Case%20LVNetwork.pdf.
[30] Divshali, P. H., A. Alimardani, S. H. Hosseinian, and M. Abedi. "Decentralized cooperative control strategy of microsources for stabilizing autonomous VSC-based microgrids." *IEEE transactions on power systems*27, no. 4 (2012): 1949-1959.
[31] Terzija, V. V. "Adaptive underfrequency load shedding based on the magnitude of the disturbance estimation." *IEEE Transactions on power Systems* 21, no. 3 (2006): 1260-1266.
[32] Sigrist, L., I. Egido, and L. Rouco. "A method for the design of UFLS schemes of small isolated power systems." *IEEE Transactions on Power Systems* 27, no. 2 (2012): 951-958.
[33] Karimi, M., H. Mohamad, H. Mokhlis, and A. H. A. Bakar. "A new approach of under-frequency load shedding technique in an islanded distribution network." *Int Rev Electron Eng* 7, no. 2 (2012): 4155-62.
[34] Karimi, M., H. Mohamad, H. Mokhlis, and A. H. A. Bakar. "Under-frequency load shedding scheme for islanded distribution network connected with mini hydro." *International Journal of Electrical Power & Energy Systems* 42, no. 1 (2012): 127-138.
[35] ‘‘Lithium Iron Phosphate Battery,’’ LiFePO4 battery specification. Hipower New Energy Group Co., Ltd., <www.hipowergroup.com>; 2010.